J Mater Sci (2010) 45:3778–3783
DOI 10.1007/s10853-010-4431-6

An alternative approach of solid-state reaction to prepare nanocrystalline $KNbO_3$

Tingting Su · Heng Jiang · Hong Gong ·
Yuchun Zhai

Received: 29 December 2009 / Accepted: 19 March 2010 / Published online: 2 April 2010

Abstract A simple preparation of $KNbO_3$ powders was proposed by an alternative approach of solid-state reaction. Stoichiometric niobium oxalate and potassium acetate were mixed in water and then dried. It was demonstrated that an ion-exchange reaction occurred with the formation of $K[NbO(C_2O_4)_2]\cdot nH_2O$ intermediate. The single-phase $KNbO_3$ powders were synthesized when $K[NbO(C_2O_4)_2]\cdot nH_2O$ intermediate was calcined between 500 and 800 °C for 3 h. $KNbO_3$ powders obtained at 500 °C are determined as orthorhombic structure with an average particle size of 20–50 nm by X-ray diffraction, scanning electron microscope (SEM), and transmission electron microscopy (TEM) analysis. The morphologies of $KNbO_3$ obtained at different temperatures were observed by SEM and TEM analysis. The average band gap energy is estimated to be 3.16 eV by UV–vis diffuse reflectance spectra.

Introduction

Potassium niobate ($KNbO_3$) is a technologically important perovskite-type material due to its electro-optic, nonlinear optical, piezoelectric, luminescence, and photocatalytic properties [1–12]. Many wet chemical methods have been developed to prepare $KNbO_3$ powders along with the applications of $KNbO_3$ in various fields [13]. Among them, sol–gel reaction [14–18] is a successful technique to synthesize $KNbO_3$ powders. However, it must be performed at 600 °C under dry nitrogen atmosphere. As for homogeneous precipitation [19–22] and polymerized complex methods [2, 23], the synthesized $KNbO_3$ usually shows low crystallinity or undergoes a big weight loss process (>90%) after calcination at 700 °C. Hydrothermal method [5, 6, 10–12, 24–33] is a low temperature process, but the concentration of KOH solution used is as high as 8 M or more and the reaction time is several days. Although the required concentration of KOH is reduced (0.5 M) in supercritical environment, the isopropanol used is flammable, toxic and may cause pollution in glycothermal technique [34]. $KNbO_3$ powders are usually synthesized by solid-state method between K_2CO_3 and Nb_2O_5, which requires long periods of calcination at 800 °C or above [13, 35, 36]. However, the high temperature may result in the volatilization of K_2CO_3 or large particle sizes from 0.1 to several micrometers [7, 35, 36]. Furthermore, the contamination is always introduced into the high-quality ceramics during ball milling process.

The above methods for preparation of $KNbO_3$ powders are mainly focused on the formation of single-phase $KNbO_3$. In our study, we not only obtain pure $KNbO_3$ powders, but also pay more attention to the crystallinity and particle size. A facile method is performed to fabricate pure nanocrystalline $KNbO_3$ powders.

Experimental section

The starting materials for preparation of $KNbO_3$ were CH_3COOK, K_2CO_3, KNO_3, HCOOK, and Nb_2O_5. All materials were obtained from commercial sources with analytical grade. Niobium oxalate was prepared according to the procedure of Beck et al. [37]. The molecular formula

T. Su · H. Jiang (✉) · H. Gong
School of Chemistry and Materials Science, Liaoning Shihua University, Fushun 113001, People's Republic of China
e-mail: hjiang78@hotmail.com

T. Su · Y. Zhai
School of Materials Science and Metallurgy, Northeastern University, Shenyang 110005, People's Republic of China

of the recrystallized niobium oxalate was determined as $NH_4[NbO(C_2O_4)_2(H_2O)_2](H_2O)_3$ by XRD analysis, which matched well with the standard data (JCPDS 83-1993). Considering the hygroscopic property, the water content of CH_3COOK and K_2CO_3 powders was measured by thermogravimetric (TG) analysis before use.

The stoichiometric amounts (the molar ratio of K:Nb is 1:1) of CH_3COOK (10.63 g, H_2O content is 12.44% by TG analysis) and niobium oxalate ($NH_4[NbO(C_2O_4)_2(H_2O)_2]$ $(H_2O)_3$, 39.01 g, Nb_2O_5 content is 32.30% by TG analysis) were ground in an agate mortar and pestled in 8.0 mL water. The mixed slurry was ground for 1–2 h under IR lamp till water was vaporized. Small amounts of CH_3COOH and NH_3 were released simultaneously during the grinding process. The mixture was heated in a corundum crucible at 500, 600, 700, and 800 °C for 3 h, respectively. These obtained samples were named as KANO5, KANO6, KANO7, and KANO8, respectively. For the sake of comparison, stoichiometric mixture of CH_3COOK and niobium oxalate was mixed without water and followed by calcining at 500 °C for 3 h.

The other controlled experiments were carried out by using different potassium and niobium reactants as raw materials, which follow the same procedure as described for KANO samples. A stoichiometric mixture of CH_3 COOK and Nb_2O_5 with 1:1 M ratio of K:Nb was mixed with water and then dried. The mixture was calcined in the range from 500 to 800 °C for 3 h, respectively. These obtained samples were named as KAN5, KAN6, KAN7, and KAN8, respectively. Mix the stoichiometric raw materials of K_2CO_3 and niobium oxalate with water. Heat the dried mixture between 500 and 800 °C for 3 h and name them as KCNO5-8, respectively. A stoichiometric mixture of KNO_3 and niobium oxalate was mixed with water and then dried. The mixture was calcined in the range from 500 to 800 °C for 3 h and named as KNNO5-8, respectively. A stoichiometric mixture of HCOOK and niobium oxalate was calcined between 500 and 800 °C for 3 h. These obtained products were named as KFNO5-8, respectively.

Characterization

The structures of as-synthesized materials were confirmed by powder X-ray diffraction (XRD) using a D/MAX-RB X-ray diffractometer (XRD, Rigaku, Japan) with graphite monochromater and Cu$K\alpha$ radiation (40 kV, 100 mA). The step scan mode was performed with a step width of 0.02°, at a rate of 4° (2θ) per min. The phase indexing and lattice parameters calculation were performed by MDI Jade 5.0 software. The degree of relative crystallinity is calculated according to the total area of the diffraction peaks at 21.9°, 31.6°, 45.0°, 50.6°, and 55.9° in the XRD pattern of the samples. For KANO series samples, the powder crystalline calcined at 700 °C (KANO7) was considered to be 100% in crystallinity for the biggest area [38]. The degree of relative crystallinity was determined by comparing the total area under crystalline peaks of other samples with that of KANO7, respectively [39]. The morphologies were observed using a scanning electron microscope (SEM) (JSM-7500F-EDS). Transmission electron microscopy (TEM) observations were made with a JEM-2100 instrument at the accelerating voltage of 200 kV. All the powders were dispersed in ethanol on a carbon-coated TEM copper grid. UV–vis diffuse reflectance spectra were recorded with a Lamda 900 UV–vis-NIR spectrophotometer. The PELA-1020 Sphere Accessory is equipped with a 60 mm Spectralon® integrating sphere, transfer optics, a thermostat-regulated lead sulfide (PbS) detector, and an extended range photomultiplier tube (PMT). TG analysis was carried out on a Perkin-Elmer Pyris 1 TGA. The atmosphere was air with a flow rate of 20 mL min^{-1} at 20 K min^{-1} in the range from 30 to 800 °C. Fourier transform infrared (FTIR) spectra were obtained in KBr discs on a Perkin-Elmer Spectrum GX. Sixteen scans were co-added with a resolution of 4 cm^{-1}, in the range of 4,000–400 cm^{-1}.

Results and discussion

In conventional solid-state reaction, the raw materials are usually mixed under solvent-free condition. As a comparison, the components of CH_3COOK/niobium oxalate mixed without water were investigated by FTIR and TG analysis. FTIR spectra of CH_3COOK, niobium oxalate and CH_3COOK/niobium oxalate mixed without water are shown in Fig. 1. In Fig. 1c, peaks of CH_3COOK/niobium oxalate mixed without water are nearly the superposition of CH_3COOK (Fig. 1a) and niobium oxalate (Fig. 1b). For example, peak at 1,625 cm^{-1} is the overlapping bands of 1,574 cm^{-1} (Fig. 1a) and 1,683 cm^{-1} (Fig. 1b). The peak broadening at 1,400 cm^{-1} results from the co-action of 1,407 cm^{-1} (Fig. 1a) and 1,397 cm^{-1} (Fig. 1b). It can be inferred that the powders are the mechanical mixture of CH_3COOK and niobium oxalate. Niobium oxalate, an excellent water-soluble complex, is insensitive to moisture and easily handled in ambient atmosphere [37, 40, 41]. In our study, the mixture of niobium oxalate and CH_3COOK was uniformly distributed by adding small amount of water. The FTIR spectrum of CH_3COOK/niobium oxalate mixed with water is shown in Fig. 1d. In Fig. 1a, peaks at 1,574 and 1,407 cm^{-1} are attributed to the stretch vibration of C=O and C–O, respectively. As shown in Fig. 1d, the disappearance of the peaks of CH_3COO^- indicates that CH_3COOK has reacted completely after

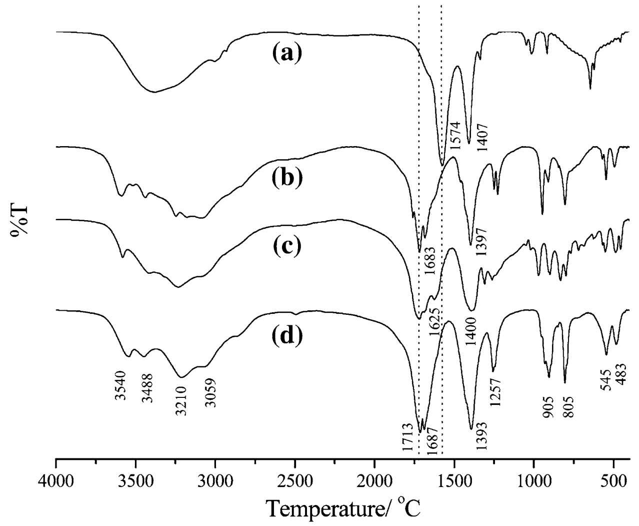

Fig. 1 FTIR spectra of *a* CH_3COOK, *b* niobium oxalate, *c* CH_3COOK/niobium oxalate mixed without water, and *d* CH_3COOK/niobium oxalate mixed with water

mixing CH_3COOK and niobium oxalate in water. It can be inferred from the above IR analysis that an irreversible ion-exchange reaction between NH_4^+ and K^+ occurs when the raw materials are ground in water. Part of CH_3COONH_4 obtained is hydrolyzed in the presence of water to form CH_3COOH and $NH_3{\cdot}H_2O$ as shown below. Small amount of CH_3COOH and NH_3 was released when water was evaporated during mixing:

$$\mathrm{NH_4[NbO(C_2O_4)_2(H_2O)_2](H_2O)_3 + CH_3COO}K \rightarrow \mathrm{K[NbO(C_2O_4)_2]} \cdot n\mathrm{H_2O} + \mathrm{CH_3COONH_4} + (5-n)\mathrm{H_2O}, \tag{1}$$

$$\mathrm{CH_3COONH_4 + H_2O \rightleftharpoons CH_3COOH \uparrow + NH_3 \cdot H_2O \uparrow} . \tag{2}$$

The absorption bands at approximately 3,540 and 3,448 cm^{-1} are attributed to OH vibration. Peaks at 3,210 and 3,059 cm^{-1} result from the residual NH_4^+. The C=O stretch vibration at 1,713, 1,687 cm^{-1} and C–O at 1,393, 1,257 cm^{-1} can be observed. Bands at 905 and 805 cm^{-1} are assigned to COO^-. 545 and 483 cm^{-1} bands are the result of M–O stretch vibration.

TG curves of CH_3COOK, niobium oxalate, CH_3COOK/niobium oxalate mixed without water, and CH_3COOK/niobium oxalate mixed with water are shown in Fig. 2. It can be seen from Fig. 2a–c, the decomposition process of the CH_3COOK/niobium oxalate mixed without water is an incorporation of CH_3COOK and niobium oxalate. Figure 2b shows that niobium oxalate decomposes to niobic acid ($Nb_2O_5{\cdot}xH_2O$) at about 330 °C and then yields Nb_2O_5 at 620 °C [42]. In Fig. 2d, the weight loss between 50 and 500 °C is the decomposition process of the $K[NbO(C_2O_4)_2]{\cdot}nH_2O$ intermediate. There is no weight loss above 500 °C, which is different from Fig. 2c. TG analysis of the $K[NbO(C_2O_4)_2]{\cdot}nH_2O$ precursor shows a 57.0% weight loss rate from 50 to 500 °C (Fig. 2d).

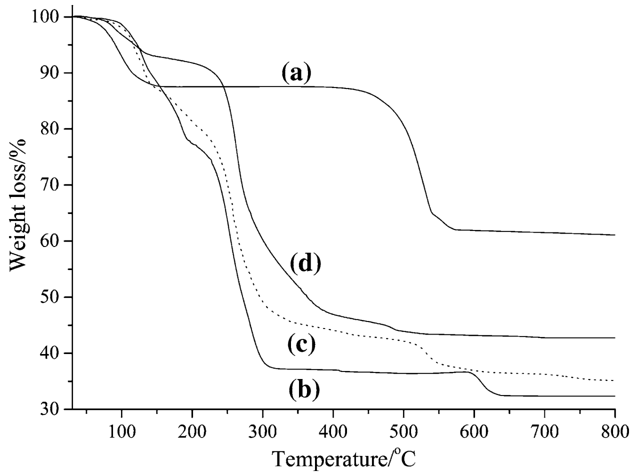

Fig. 2 TG results of *a* CH_3COOK, *b* niobium oxalate, *c* CH_3COOK/niobium oxalate mixed without water, and *d* CH_3COOK/niobium oxalate mixed with water

If niobium oxalate and K_2CO_3 are mixed with water, larger amount of bubble is evolved. FTIR and TG analysis results (which are not shown here) show that the ion-exchange reaction occurs according to Eqs. 3 and 4:

$$\mathrm{2NH_4[NbO(C_2O_4)_2(H_2O)_2](H_2O)_3 + K_2CO_3} \rightarrow \mathrm{2K[NbO(C_2O_4)_2]} \cdot n\mathrm{H_2O} + \mathrm{(NH_4)_2CO_3} + 2(5-n)\mathrm{H_2O}, \tag{3}$$

$$\mathrm{(NH_4)_2CO_3 \rightarrow 2NH_3 \uparrow + CO_2 \uparrow + H_2O}. \tag{4}$$

For the sake of comparison, stoichiometric CH_3COOK and niobium oxalate were mixed without water and then calcined at 500 °C for 3 h. The XRD result is shown in Fig. 3.

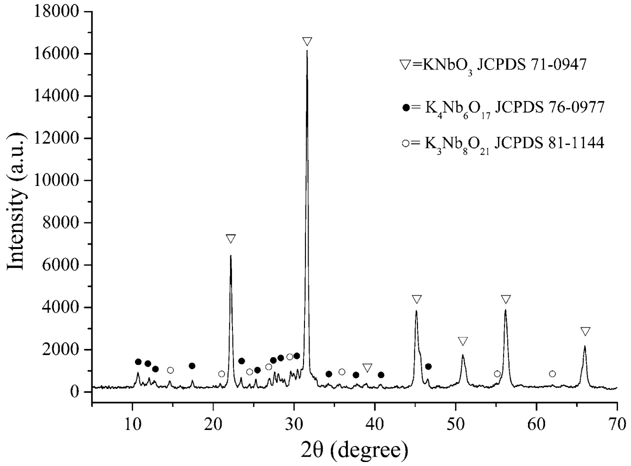

Fig. 3 XRD powder diffraction patterns of CH_3COOK/niobium oxalate mixed without water and calcined at 500 °C for 3 h

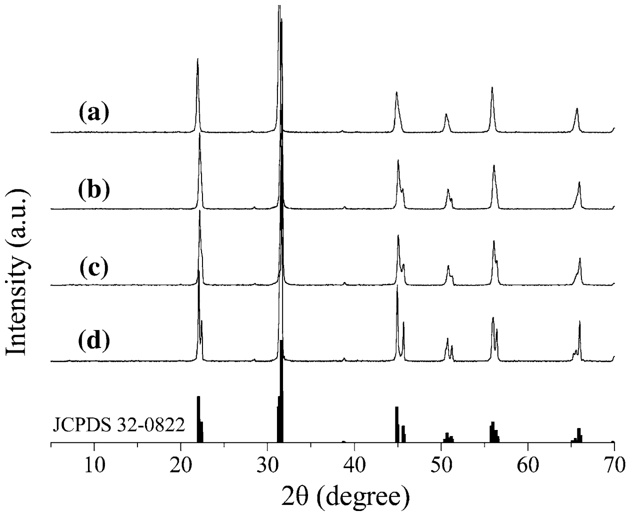

Fig. 4 XRD powder diffraction patterns of *a* KANO5; *b* KANO6; *c* KANO7; *d* KANO8. As a reference, the pattern of standard JCPDS 32-0822 is shown at the *bottom*

Although $KNbO_3$ phase can be obtained, the impurity phase $K_4Nb_6O_{17}$ and $K_3Nb_8O_{21}$ can be observed.

Figure 4a–d show the XRD patterns of the KANO series samples, which can be identified and indexed using the standard XRD data. All materials show perovskite-type diffraction patterns and all diffraction peaks are accordant with orthorhombic structure $KNbO_3$ (JCPDS 32-0822, Fig. 4). In the case of KANO5 powders, the broadening of peaks at 21.9°, 45.0°, 50.6°, 55.9°, and 65.7° is due to the small particle sizes, which can be testified by XRD, SEM, and TEM analysis later. The average particle size of $KNbO_3$ calcined at 500 °C is estimated to be about 41 nm using the Scherrer's equation. The calculated lattice parameters $a = 5.69536$ Å (0.001093), $b = 5.71322$ Å (0.001586), and $c = 3.97496$ Å (0.001026) for KANO8 are well consistent with the values from the standard card $a = 5.6950$ Å, $b = 5.7213$ Å, and $c = 3.9739$ Å (JCPDS 32-0822). There are a few differences in the calculated lattice parameters from standard card values, which may be attributed to the change in preparative conditions, such as calcination temperature.

On the basis of experimental data, it has been found that a single-phase $KNbO_3$ can be produced by heating $K[NbO(C_2O_4)_2]\cdot nH_2O$ precursor in the temperature range from 500 to 800 °C for 3 h. Table 1 shows the XRD results of various other starting materials calcined at different temperatures. It can be inferred that the activity of niobic acid decomposed by the precursor in situ is higher than that of Nb_2O_5 reagent. The conclusion has been confirmed by the reaction of Nb_2O_5 with CH_3COOK in the same

Table 1 The summary of XRD results of KANO, KAN, KCNO, KNNO and KFNO series samples

Sample	Starting materials	Product color	Components of final product	Degree of relative crystallinity (%)
KANO5	Niobium oxalate + CH_3COOK	Bluish-gray	Orthorhombic $KNbO_3$	85.7
KANO6		Bluish-gray	Orthorhombic $KNbO_3$	95.3
KANO7		Bluish-gray	Orthorhombic $KNbO_3$	100
KANO8		White	Orthorhombic $KNbO_3$	97.5
KAN5	Nb_2O_5 + CH_3COOK	White	Orthorhombic $KNbO_3$ + $K_4Nb_6O_{17}^{a}$	–
KAN6		White	Orthorhombic $KNbO_3$ + $K_4Nb_6O_{17}^{a}$	–
KAN7		White	Orthorhombic $KNbO_3$ + $K_4Nb_6O_{17}^{b}$	–
KAN8		White	Orthorhombic $KNbO_3$ + $K_4Nb_6O_{17}^{b}$	–
KCNO5	Niobium oxalate + K_2CO_3	White	Orthorhombic $KNbO_3$	88.1
KCNO6		White	Orthorhombic $KNbO_3$	100
KCNO7		White	Orthorhombic $KNbO_3$	89.9
KCNO8		White	Orthorhombic $KNbO_3$	92.0
KNNO5	Niobium oxalate + KNO_3	Bluish-gray	Amorphous and $KNbO_3^{a}$	–
KNNO6		Bluish-gray	Orthorhombic $KNbO_3$	97.9
KNNO7		Grayish-white	Orthorhombic $KNbO_3$	100
KNNO8		Slight yellow	Orthorhombic $KNbO_3$	98.6
KFNO5	Niobium oxalate + HCOOK	Bluish-gray	Orthorhombic $KNbO_3$	87.3
KFNO6		Bluish-gray	Orthorhombic $KNbO_3$	93.6
KFNO7		Bluish-gray	Orthorhombic $KNbO_3$	99.6
KFNO8		White	Orthorhombic $KNbO_3$	100

[a] Small

[b] Trace

condition as KANO, which is listed in Table 1. In the cases of KAN series samples, the secondary phase ($K_4Nb_6O_{17}$) appears and prevents the crystallization of single-phase $KNbO_3$. The colors of KANO5-7 are bluelish-gray and their average particle sizes are smaller compared with KAN series samples. However, the colors of KCNO5-8 are white and their average particle sizes are larger with a lower relative crystallinity when niobium oxalate reacts with K_2CO_3. In the case of the mixture of niobium oxalate and KNO_3, KNNO5 contains amorphous phase since KNO_3 cannot be decomposed completely at 500 °C. The products obtained using HCOOK and niobium oxalate as raw materials are similar to KANO5-8.

The SEM image of KANO5 powders is given in Fig. 5a, where the inset is a representative TEM image. The aggregation of nanometer-sized fine particles is clearly observed in the SEM and TEM images. About 80% of these particles have an average particle size of 20–50 nm. SEM images of $KNbO_3$ powders obtained at 600, 700, and 800 °C are shown in Fig. 5b–d. $KNbO_3$ particles formed are well-crystallized and exhibit ladder-shaped cuboid morphology with the increase of calcination temperature. The high calcination temperature improves the crystallization process and the crystal grain growth, thus resulting in particles with regular shape and high crystallinity. In addition, it can be found that the particle sizes of KANO6-8 increase with the rise of calcination temperature. The inset of Fig. 5d displays the TEM image of KANO8. The average particle sizes of the powders fabricated at 800 °C are estimated to be about 200–300 nm in width and several hundreds nanometers in length. About 90% of the cubes are estimated to be 300–500 nm in height.

The UV–vis diffuse reflectance spectra of KANO series samples are as shown in Fig. 6. The band gap absorption edge of KANO5-8 samples is estimated as 392, 386, 399, and 393 nm, respectively. The result shows that it is no correlation between absorption edge and calcination temperature. The average value of them is about 392.5 nm. The corresponding band gap energy is determined as 3.16 eV by the following Eq. 5 [43]:

$$\lambda\ (\mathrm{nm}) = 1{,}240/\mathrm{Eg}\ (\mathrm{eV}), \qquad (5)$$

where Eg denotes the energy gap of semiconductor and λ denotes the band gap absorption edge.

The average band gap energy obtained is similar to that of $KNbO_3$ nanocubes (3.14 eV) [11]. The valence band and conduction band of $KNbO_3$ are composed of O_{2p} and Nb_{4d} orbital, respectively. The absorption curves have a steep

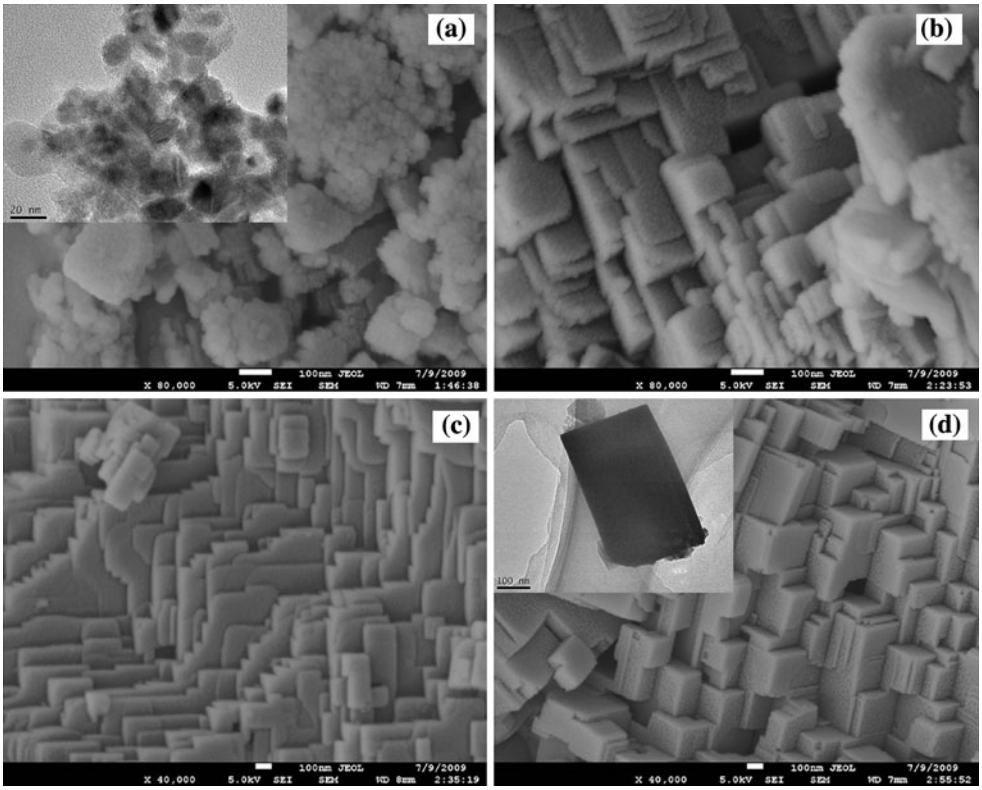

Fig. 5 **a** SEM image of KANO5. The *inset* displays a representative TEM image with 20 nm scale. **b** SEM image of KANO6. **c** SEM image of KANO7. **d** SEM image of KANO8. The *inset* displays a representative TEM image with 100 nm scale

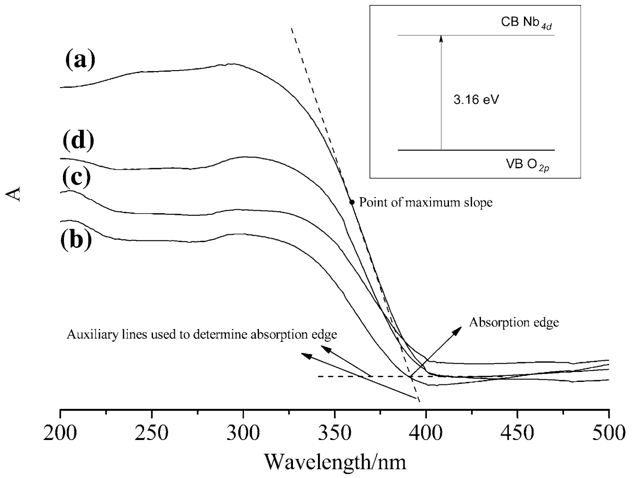

Fig. 6 UV–vis diffused reflectance spectra of the as-synthesized: *a* KANO5; *b* KANO6, *c* KANO7, and *d* KANO8

edge for all the samples, which indicate that the UV light absorption is due to the band-to-band transition from O_{2p} to Nb_{4d} directly (as shown in Fig. 6 inset).

Conclusions

In the alternative approach of solid-state method, an ion-exchange reaction between NH_4^+ and K^+ occurs when niobium oxalate and CH_3COOK are ground in water. The perovskite $KNbO_3$ was successfully prepared by calcining $K[NbO(C_2O_4)_2]\cdot nH_2O$ precursor at 500, 600, 700, and 800 °C for 3 h, respectively. XRD analysis shows the obtained $KNbO_3$ particles have orthorhombic structure. The average particle size of $KNbO_3$ obtained at 500 °C is about 41 nm. The raw materials of niobium oxalate and CH_3COOK are excellent water-soluble complex. The raw materials were adjusted to uniformly distribute in slurry by adding water instead of the ball milling process, which avoided the interfusion of contamination to $KNbO_3$ powders. The average band gap absorption edge of the catalyst $KNbO_3$ is determined to be 392.5 nm. The band gap energy of $KNbO_3$ at different calcination temperatures was estimated to be average of 3.16 eV from the onset of UV–vis diffuse reflectance spectra.

References

1. Saito Y, Takao H, Tani T, Nonoyama T, Takatori K, Homma T, Nagaya T, Nakamura M (2004) Nature 432:84
2. Pribošič I, Makovec D, Drofenik M (2005) Chem Mater 17:2953
3. Meng XY (2007) J Appl Phys 101:103506
4. Sastry PU (2002) Solid State Commun 122:41
5. Li B, Hakuta Y, Hayashi H (2005) J Supercrit Fluids 35:254
6. Lu CH, Lo SY, Lin HC (1998) Mater Lett 34:172
7. Nagata H, Matsumoto K, Hirosue T, Hiruma Y, Takenaka T (2007) Jpn J Appl Phys 46:7084
8. Wiegel M, Emond MHJ, Stobbe ER, Blasse G (1994) J Phys Chem Solids 55:773
9. Pankratov V, Grigorjeva L, Millers D, Corradi G, Polgàr K (2000) Ferroelectrics 239:241
10. Ding QP, Yuan YP, Xiong X, Li RP, Huang HB, Li ZS, Yu T, Zou ZG, Yang SG (2008) J Phys Chem C 112:18846
11. Liu JW, Chen G, Li ZH, Zhang ZG (2007) Int J Hydrogen Energy 32:2269
12. Hayashi H, Hakuta Y, Kurata Y (2004) J Mater Chem 14:2046
13. Choi J, Ryu SY, Balcerski W, Lee TK, Hoffmann MR (2008) J Mater Chem 18:2371
14. Tanaka K, Kakimoto K, Ohsato H (2007) J Eur Ceram Soc 27:3591
15. Nazeri-eshghi A, Kuang AX, Mackenzie JD (1990) J Mater Sci 25:3333. doi:10.1007/BF00587695
16. Amini MM, Sacks MD (1991) J Am Ceram Soc 74:53
17. Amini MM, Mirzaee M (2009) Ceram Int 35:2367
18. Yogo T, Banno K, Sakamoto W, Hirano S (2003) J Mater Res 18:1679
19. Muthurajan H, Kumar HH, Samuel V, Gupta UN, Ravi V (2008) Ceram Int 34:671
20. Kim MJ, Matijević E (1992) J Mater Res 7:912
21. Bhattacharyya K, Tyagi AK (2009) J Alloys Compd 470:580
22. Kakimoto K, Ito T, Ohsato H (2008) Jpn J Appl Phys 47:7669
23. Lin Y, Yang HB, Zhu JF, Wang F, Luo HJ (2008) Mater Manuf Processes 23:796
24. Wohlrab S, Weiss M, Du H, Kaskel S (2006) Chem Mater 18:4227
25. Hana XY, Zhang DM, Zhong ZC, Yang FX, Wei N, Zheng KY, Li ZH, Gao YH (2008) J Phys Chem Solids 69:193
26. Ishikawa M, Kadota Y, Takiguchi N, Hosaka H, Morita T (2008) Jpn J Appl Phys 47:7673
27. Liu JF, Li XL, Li YD (2003) J Cryst Growth 247:419
28. Suyal G, Colla E, Gysel R, Cantoni M, Setter N (2004) Nano Lett 4:1339
29. Magrez A, Vasco E, Seo JW, Dieker C, Setter N, Forró L (2006) J Phys Chem B 110:58
30. Vasco E, Magrez A, Forro L, Setter N (2005) J Phys Chem B 109:14331
31. Goha GKL, Lange FF (2003) J Mater Res 18:338
32. Ishikawa M, Takiguchi N, Hosaka H, Morita T (2008) Jpn J Appl Phys 47:3824
33. Paula AJ, Parra R, Zaghete MA, Varela JA (2008) Mater Lett 62:2581
34. Lu CH, Lo SY, Wang YL (2002) Mater Lett 55:121
35. Komatsu R, Adachi K, Ikeda K (2001) Jpn J Appl Phys 40:5657
36. Fang TH, Hsiao YJ, Chang YS, Chang YH (2006) Mater Chem Phys 100:418
37. Beck K, Seyeda H, Sulkowski U, Rosenkranz A (2007) US Patent 7 241 911, 10 July 2007
38. Nobre MAL, Longo E, Leite ER, Varela JA (1996) Mater Lett 28:215
39. Kamat MS, Osawa T, DeAngelis RJ, Koyama Y, DeLuca PP (1988) Pharm Res 5(7):426
40. Emerson RC, Masato K (2001) Chem Mater 13:1905
41. Asai T, Camargo ER, Kakihana M, Osada M (2000) J Alloys Compd 309:113
42. Su TT, Zhai YC, Jiang H, Gong H (2009) J Therm Anal Calorim 98:449
43. Nakamura T, Suzuki H (1977) US Patent 4 034 396, 5 July 1977